Supporting Information

Liquid Crystalline Moiety-Assisted Perpendicular Orientation of Cylindrical Domains within P4VP-*b*-PMA(Az) Films with High Aspect Ratio

Ting Qu,[a] Song Guan,[a] Chen Zhang,[a] Xiaoxiong Zheng,[a] Yongbin Zhao,[b] Aihua Chen[ac]*

[a.] School of Materials Science and Engineering, Beihang University, Beijing, 100191, P. R. China.

[b.] Shandong Oubo New Material Co. Ltd, Shandong, 257088, P. R. China.

[c.] Beijing Advanced Innovation Centre for Biomedical Engineering, Beihang University, Beijing, 100191, P. R. China

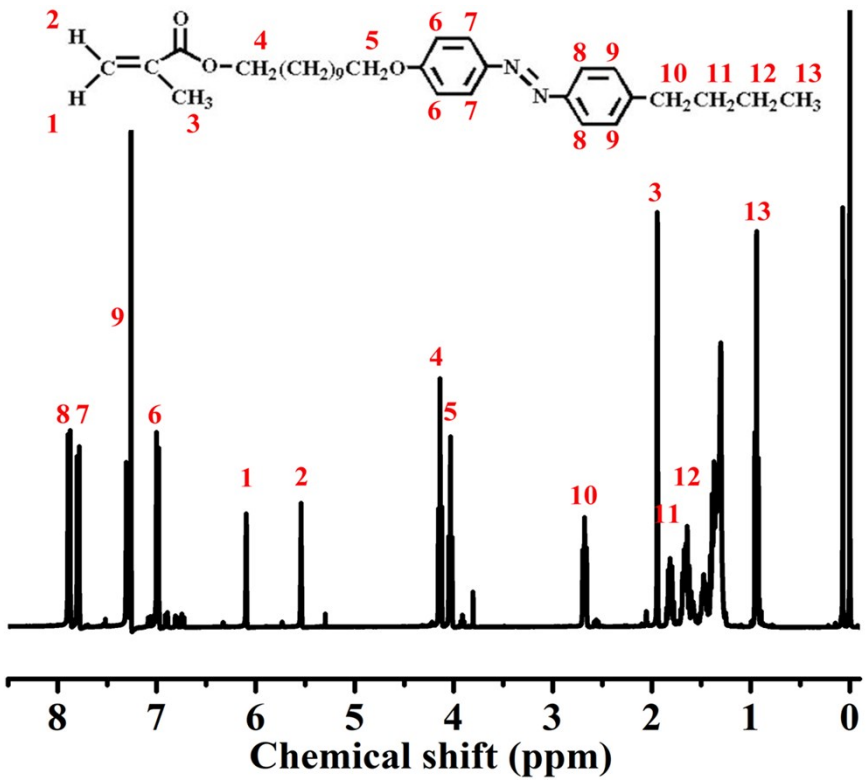

Figure S1. ^{1}H NMR spectrum of MA(Az).

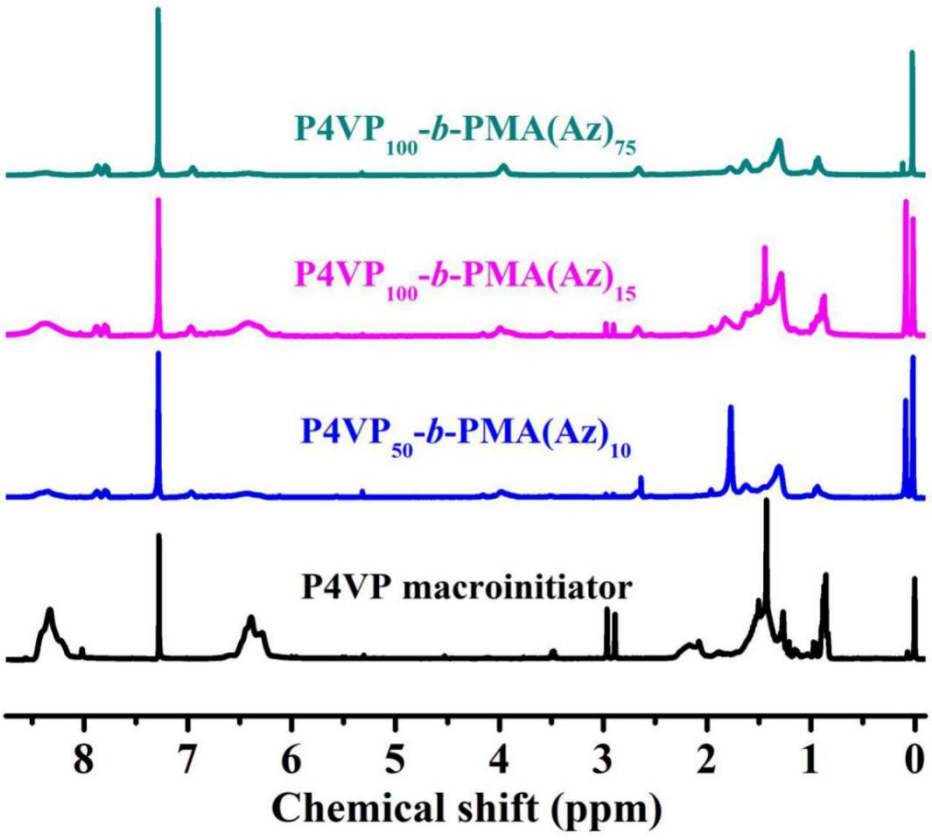

Figure S2. ^{1}H NMR spectra of different P4VP macroinitiator and P4VP$_m$-*b*-PMA(Az)$_n$ BCPs.

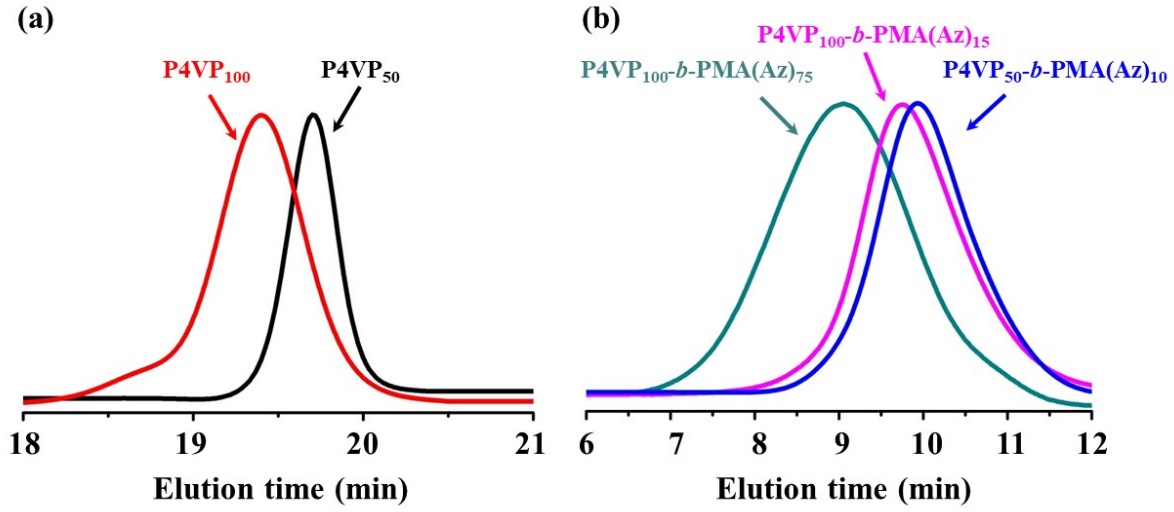

Figure S3. GPC curves of the P4VP macroinitiators with DMF as eluent, and P4VP$_m$-*b*-PMA(Az)$_n$ BCPs with THF as eluent.

Table S1. Properties of the P4VP macroinitiators and P4VP-*b*-PMA(Az) BCPs synthesized by the ATRP method.

Sample	[a]M_n (NMR)	[b]M_n (GPC)	[c]M_w/M_n	[d]DP_{P4VP}	[e]$DP_{PMA(Az)}$	[f]f_{P4VP}	[g]Morphology
P4VP$_{50}$	5,500	7,500	1.05	50	—	1	—

$P4VP_{100}$	10,500	12,500	1.12	100	—	1	—
$P4VP_{100}$-*b*-$MA(Az)_{15}$	17,880	20,660	1.28	100	15	0.58	sphere
$P4VP_{50}$-*b*-$MA(Az)_{10}$	10,180	13,800	1.28	50	10	0.50	lamellae
$P4VP_{100}$-*b*-$MA(Az)_{60}$	40,020	53,400	1.30	100	60	0.25	cylinder
$P4VP_{100}$-*b*-$MA(Az)_{75}$	47,400	60,300	1.33	100	75	0.21	sphere

[a]Number-average molecular weight determined by NMR.

[b]Number-average molecular weight determined by GPC.

[c]Polydispersity determined by GPC calibrated with polystyrene standards.

[d]Polymerization degree of P4VP.

[e]Polymerization degree of PMA(Az).

[f]The volume fraction of P4VP calculated by using molecular weight and density (P4VP: 1.15 g/cm^3 and PMA(Az): 1.10 g/cm^3) of each block.

[g]The morphology of block copolymer film is determined by SEM observations.

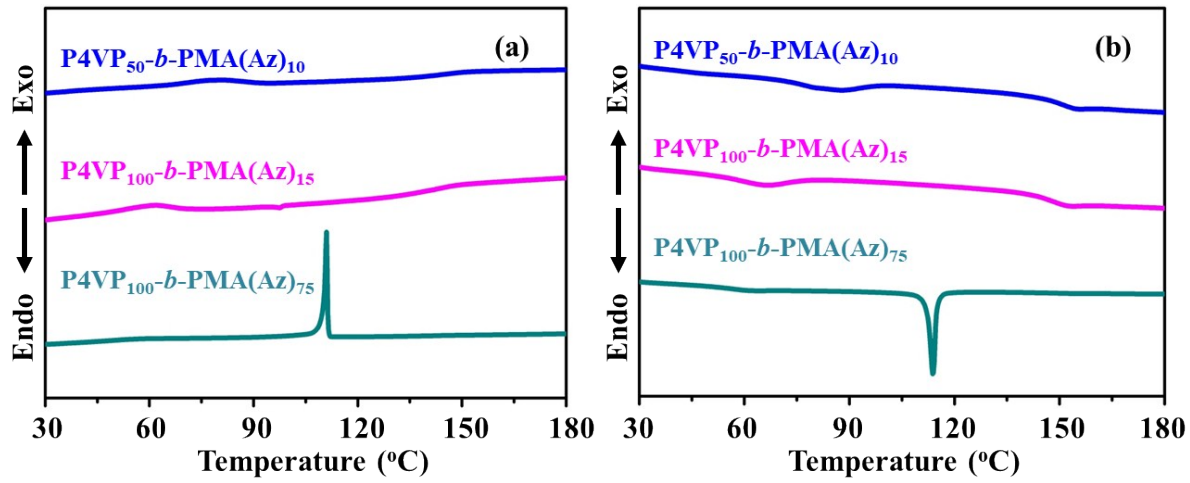

Figure S4. DSC curves of BCPs on first cooling (a) and second heating processes (b) with heating/cooling rate of ± 10 °C min^{-1}.

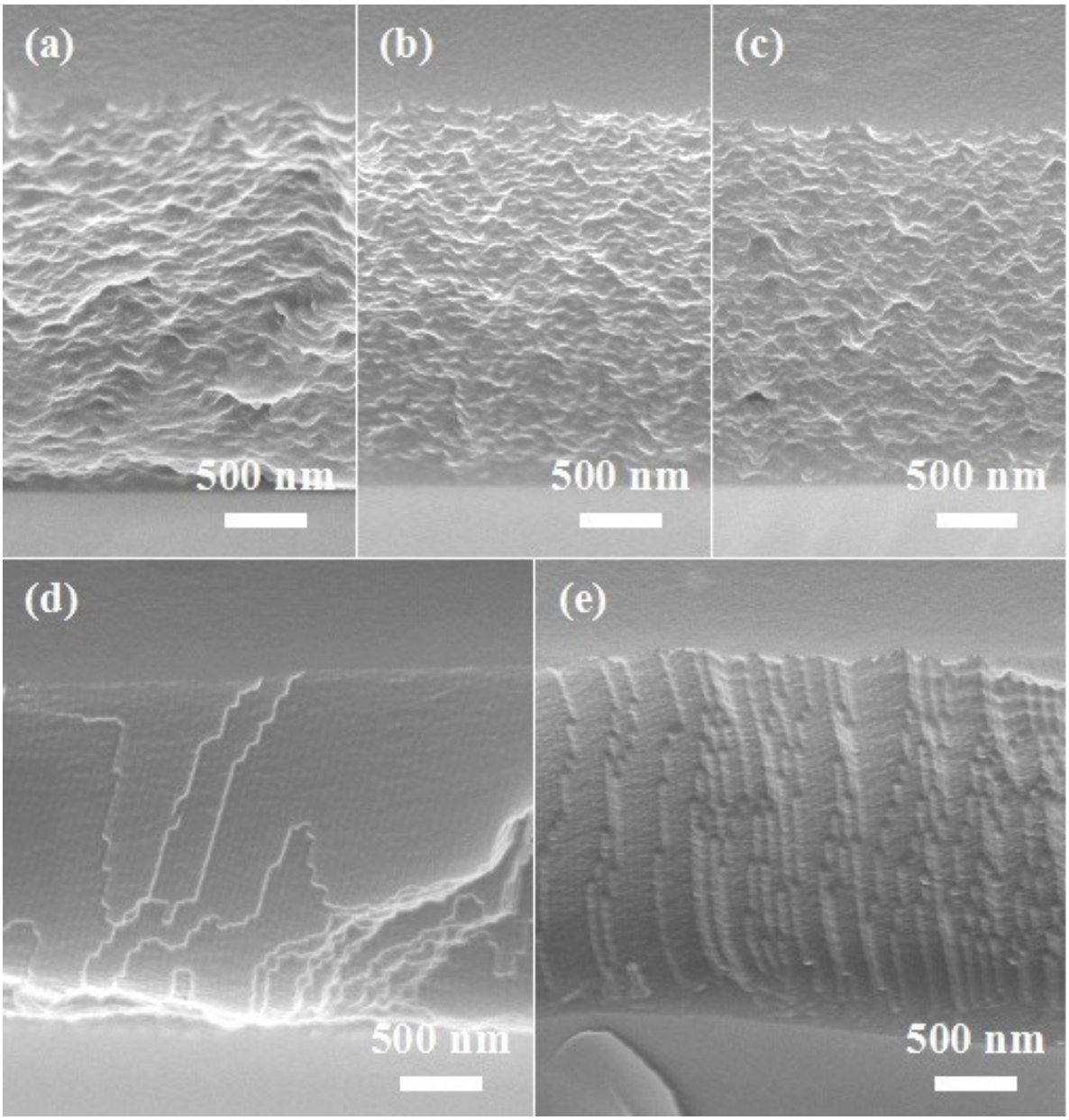

Figure S5. SEM images of $P4VP_{100}$-*b*-$PMA(Az)_{60}$ self-assembled films with 2 μm by thermal annealing (160 °C/1 h and 105 °C/24 h) (a), solvent-annealed in THF vapor (b), IPA vapor (c) and chloroform vapor (d, e) at room temperature for 24 h. d with (10) planes of hexagonal alignment, e with (11) planes of hexagonal alignment, respectively.

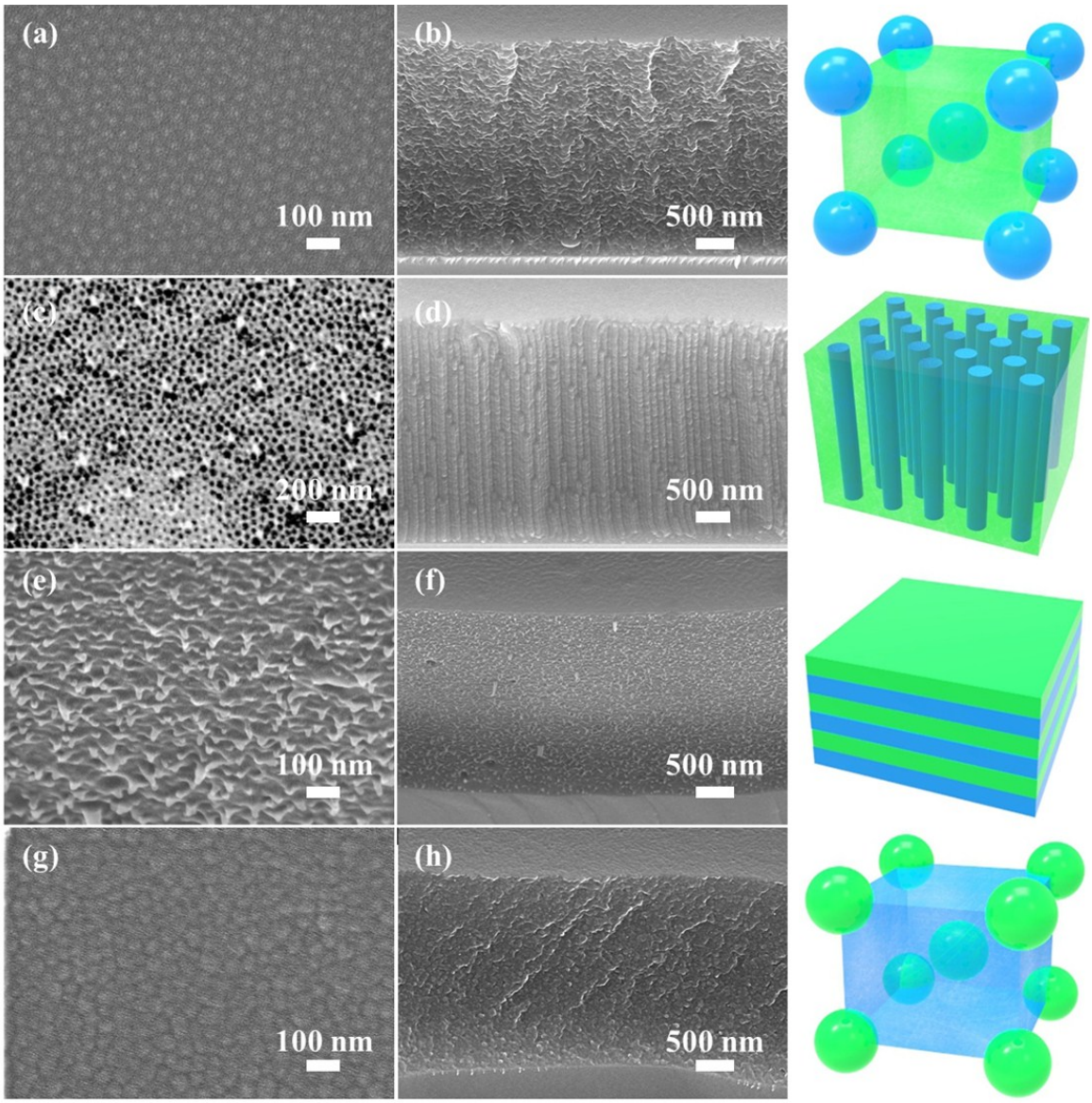

Figure S6. SEM (a, b, d-h) and AFM (c) images of $P4VP_m$-*b*-$PMA(Az)_n$ self-assembled films with different f_{P4VP}, respectively. (a, b) $P4VP_{100}$-*b*-$PMA(Az)_{75}$ (f_{P4VP} = 0.21), (c, d) $P4VP_{100}$-*b*-$PMA(Az)_{60}$ (f_{P4VP} = 0.25), (e, f) $P4VP_{50}$-*b*-$PMA(Az)_{10}$ (f_{P4VP} = 0.50), (g, h) $P4VP_{100}$-*b*-$PMA(Az)_{15}$ (f_{P4VP} = 0.58). Right images are the schemes of these morphologies, respectively. Blue part and green part represent P4VP and PMA(Az) blocks, respectively.

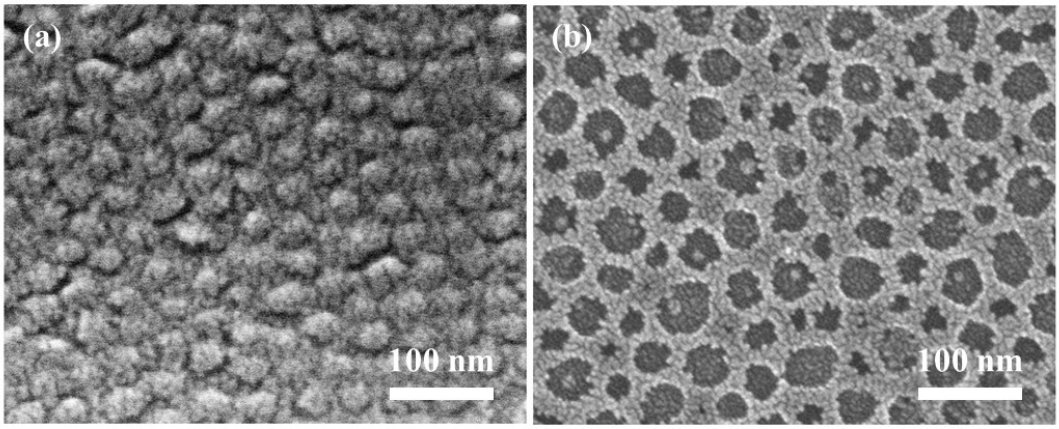

Figure S7. SEM images of the TiO_2 nanomaterials from corresponding templates: (a) top-view of TiO_2 nanosphericals from the annealed $P4VP_{100}$-*b*-$PMA(Az)_{75}$ film with 50 nm thickness; (b) top-view of TiO_2 porous films from the annealed $P4VP_{100}$-*b*-$PMA(Az)_{15}$ film with 50 nm thickness.

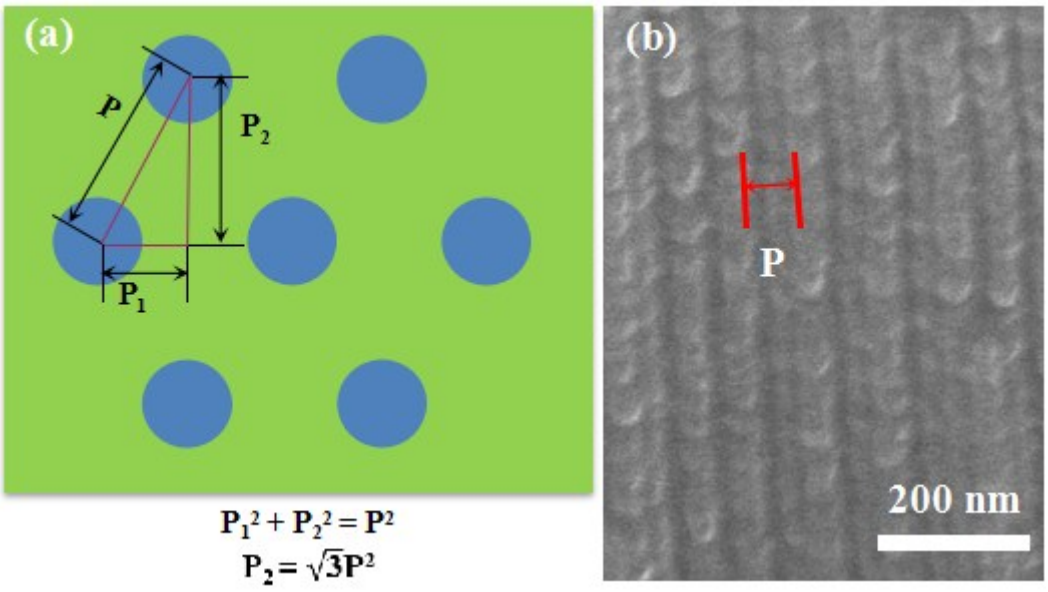

Figure S8. (a) Geometrical relationship and center-to-center distances of perpendicular cylinders, wide stripes P and narrow stripes P1. (b) SEM image of (11) planes of hexagonal alignment.

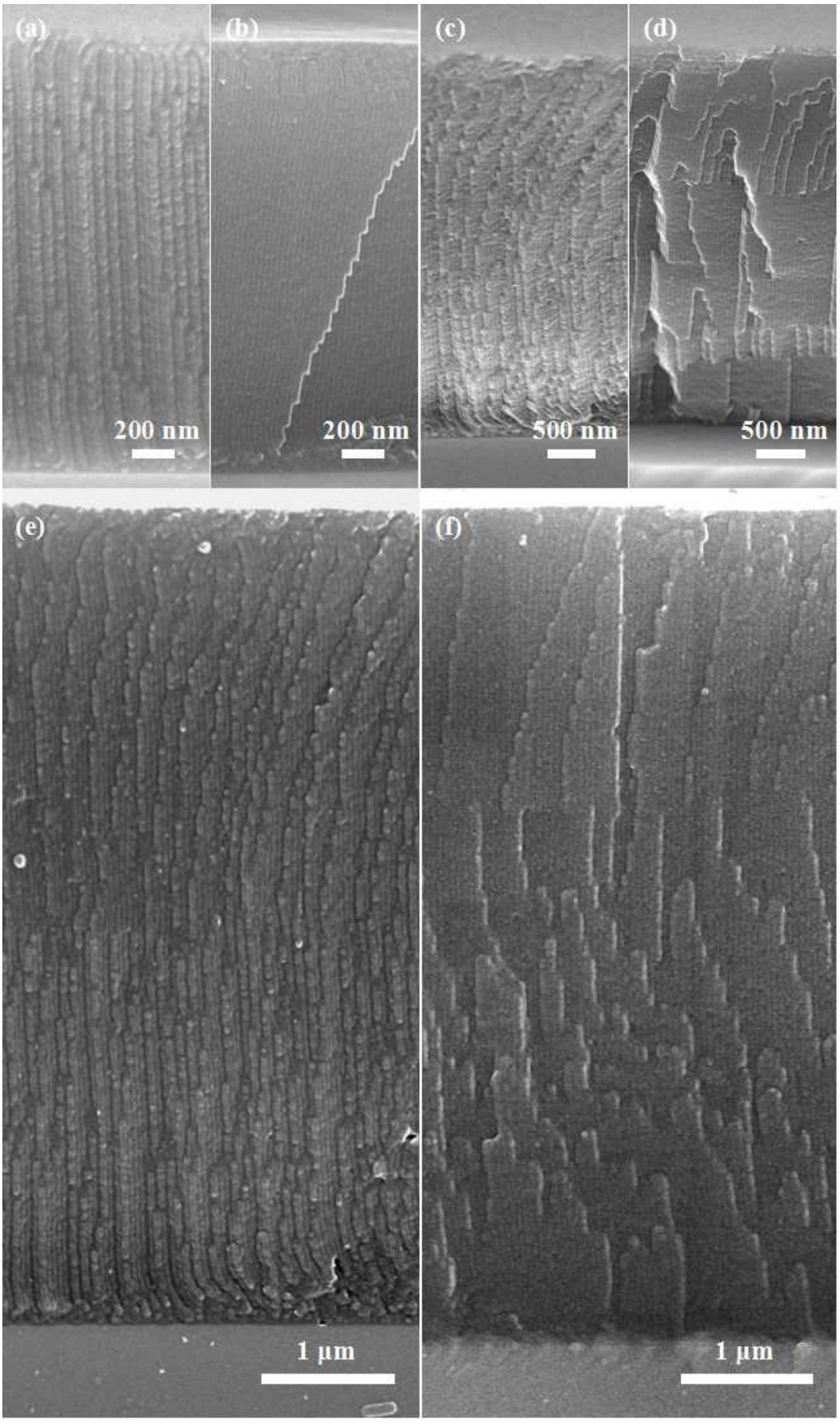
(a)
200 nm
(b)
200 nm
(c)
500 nm
(d)
500 nm
(e)
1 µm
(f)
1 µm

Figure S9. Cross-section SEM images of the solvent-annealed $P4VP_{100}$-*b*-$PMA(Az)_{60}$ films with different thicknesses: 3 μm (a, b); 4 μm (c, d); 6 μm (e, f); a, c, e with (11) planes of hexagonal alignment; b, d, f with (10) planes of hexagonal alignment, respectively.